JOURNAL OF SOLID STATE CHEMISTRY **122,** 118–129 (1996)
ARTICLE NO. 0091

Cation Distribution and Magnetic Interactions in Substituted Iron-Containing Garnets: Characterization by Iron-57 Mössbauer Spectroscopy

Frank J. Berry,*[,1] Juan Z. Dávalos,† J. Ramón Gancedo,† Colin Greaves,‡ José F. Marco,† Peter Slater,‡ and Muga Vithal*

*Department of Chemistry, The Open University, Milton Keynes MK7 6AA, United Kingdom; †Instituto de Química-Física "Rocasolano", Consejo Superior de Investigaciones Científicas, Serrano 119, 28006 Madrid, Spain; and ‡School of Chemistry, University of Birmingham, Edgbaston, Birmingham, B15 2TT, United Kingdom

Received June 8, 1995; in revised form November 1, 1995; accepted November 8, 1995

Some new compounds with garnet-related structures have been examined by ^{57}Fe Mössbauer spectroscopy. The results show that in compounds of the type $YCa_2SbFe_{4-x}Ga_xO_{12}$ ($x = 2, 3$) the gallium is distributed over both the octahedral and tetrahedral sites. In these compounds, together with materials of composition $Y_{3-2x}Ca_{2x}Sb_xFe_{5-x}O_{12}$ ($x = 1.25, 1.5$) and $Y_{3-x}Ca_xSn_xFe_{5-x}O_{12}$ ($x = 1, 2$), the results show evidence of more than one tetrahedral environment for the Fe^{3+} ions. The quadrupole splitting data for the Fe^{3+} ions in tetrahedral sites in some of these compounds are significantly larger than those previously reported for Fe^{3+} in tetrahedral sites in other garnets. The compounds $YCa_2SbFe_4O_{12}$ and $Y_2CaSnFe_4O_{12}$ magnetically order at similar temperatures and show comparable octahedral- and tetrahedral-hyperfine magnetic fields at 18 K. The substitution of Fe^{3+} by diamagnetic Sb^{5+} on the octahedral sites results in a considerable lowering of the magnetic ordering temperature. The compounds $Y_{0.5}Ca_{2.5}Sb_{1.25}Fe_{3.75}O_{12}$ and $Ca_3Sb_{1.5}Fe_{3.5}O_{12}$ show magnetic ordering on both the octahedral and tetrahedral sublattices at 18 K. A similar effect is observed in the compound $YCa_2SbFe_3GaO_{12}$ where 33% of the Fe^{3+} ions located at the tetrahedral sites are substituted by diamagnetic Ga^{3+} ions. The importance of *a–d* antiferromagnetic superexchange interactions is demonstrated in compounds of the type $YCa_2SbFe_2Ga_2O_{12}$ and $YCa_2SbFeGa_3O_{12}$ where the Ga^{3+} ions substitute the Fe^{3+} ions on both the octahedral and tetrahedral sites. In these compounds the dilution of the magnetic ions at the tetrahedral sites results in the frustration of magnetic ordering on both the *d*- and *a*-sublattices. The compound $YCa_2Sn_2Fe_3O_{12}$ which does not contain Fe^{3+} on the octahedral sites shows magnetic ordering on the *d*-sublattice in the absence of magnetic ions on the *a* sublattice. The result demonstrates the importance of *d–d* antiferromagnetic superexchange interactions.

INTRODUCTION

The synthetic garnets have the general formula $X_3Y_2Z_3O_{12}$, and X, Y, and Z represent cations with dodecahedral (c sites), octahedral (a sites), and tetrahedral (d sites) coordination, respectively. The Y and Z polyhedra share corners to form a cubic framework structure in which each octahedron is surrounded by six tetrahedra, with each tetrahedron being linked by four octahedra. The X cations occupy sites in the channels within this framework. The structure is amenable to substitution at the c, a, and d sites and a large variety of cations can be accommodated in these positions (1).

Rare earth iron garnets and in particular the yttrium iron garnet (YIG) have been extensively studied (2) due to their interesting magnetic properties. In YIG, ($Y_3Fe_5O_{12}$), both octahedral and tetrahedral sites are occupied by Fe^{3+} ions. The strongest magnetic interactions are the interlattice exchange interactions between the Fe^{3+} ions in the a and d sublattices (3), although the intrasublattice exchange interactions ($a–a$ and $d–d$) can also be important. The magnetic ordering temperature and the magnitude of the magnetic field at the iron sites of YIG can be influenced by substituting, either partially or totally, the Fe^{3+} ions at the octahedral and/or the tetrahedral sites with diamagnetic ions and/or by substituting the Y^{3+} ions at the dodecahedral sites with a magnetic rare earth ion.

It has been known for some time that Mössbauer spectroscopy is a powerful method by which iron-containing garnets can be studied (4). We report here on the synthesis of the compounds with garnet-related structures of composition $YCa_2SbFe_{4-x}Ga_xO_{12}$ ($x = 0 - 3$), $Y_{3-2x}Ca_{2x}Sb_xFe_{5-x}O_{12}$ ($x = 1.25, 1.5$), $Y_{3-x}Ca_xSn_xFe_{5-x}O_{12}$ ($x = 1, 2$), and $NaCa_2Sb_2FeGa_2O_{12}$ and their examination by ^{57}Fe Mössbauer spectroscopy.

[1] To whom correspondence should be addressed.

0022-4596/96 $18.00

EXPERIMENTAL

Compounds of composition $YCa_2SbFe_{4-x}Ga_xO_{12}$ ($x = 0 - 3$), $Y_{3-2x}Ca_{2x}Sb_xFe_{5-x}O_{12}$ ($x = 1.25, 1.5$), $Y_{3-x}Ca_xSn_xFe_{5-x}O_{12}$ ($x = 1, 2$), and $NaCa_2Sb_2FeGa_2O_{12}$, were prepared by sequential heating of appropriate proportions of $CaCO_3$, $NaNO_3$, Y_2O_3, Sb_2O_3, Fe_2O_3, Ga_2O_3, and SnO_2 at 500°C (4 h), 900°C (2 h), and finally at 1210°C (24 h) in air. It was sometimes necessary to repeat the heatings at 1210°C to obtain solids which were shown by X-ray powder diffraction to be monophasic.

^{57}Fe Mössbauer spectra were recorded at temperatures between 298 and 18 K using a helium closed-cycle cryogenerator and a constant acceleration Mössbauer spectrometer with a ^{57}Co/Rh source. Temperature control was achieved within ±1.5 K. The powdered samples were mixed with a low temperature varnish and sandwiched between aluminium foils to ensure good thermal conductivity. All the spectra were computer-fitted to Lorentzian lines using the usual constraints of equal area and width for the two lines of each doublet and of equal width and areas in the ratio 3:2:1:1:2:3 for the six lines of sextets. The spectra which were composed only of superpositioned doublets were also fitted to shape-independent distributions of quadrupole split absorptions by assuming Lorentzian profiles for the lines. The linewidths of the Lorentzian lines for the different doublets were fixed at 0.27 mms^{-1}. All the isomer shift data are referred to metallic iron. The magnetic ordering temperatures were determined by thermoscanning experiments in which the transmission of the 14.4 keV gamma rays were measured at different temperatures with the source stationary, according to procedures described elsewhere (5).

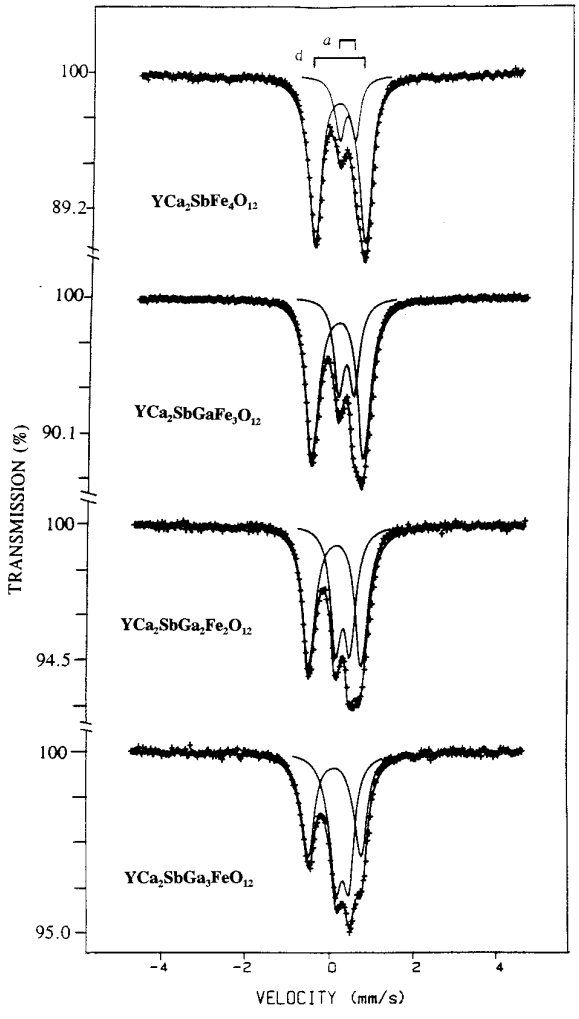

FIG. 1. Mössbauer spectra recorded at 298 K from $YCa_2SbFe_4O_{12}$, $YCa_2SbFe_3GaO_{12}$, $YCa_2SbFe_2Ga_2O_{12}$, and $YCa_2SbFeGa_3O_{12}$, and fitted to two quadrupole split absorptions.

RESULTS AND DISCUSSION

Cation Distribution

a. $YCa_2SbFe_{4-x}Ga_xO_{12}$ ($x = 0 - 3$). The ^{57}Fe Mössbauer spectra recorded at 298 K from compounds of composition $YCa_2SbFe_{4-x}Ga_xO_{12}$ ($x = 0 - 3$) are shown in Fig. 1. All the spectra were initially fitted to two quadrupole split absorptions with parameters characteristic of high-spin Fe^{3+} in octahedral and tetrahedral oxygen coordination (Table 1) and therefore consistent with the occupation by Fe^{3+} of the *a* and *d* sites. However, the fit to the spectra of the compounds with $x = 0$ and 1 gave large values of χ^2 and visual inspection of the spectra also showed large deviations of the fitted curve from the experimental points especially in the wings of the spectra. Since the linewidth of doublet *d* (0.38 mms^{-1}) was significantly larger than the linewidth of doublet *a* (0.30 mms^{-1}) a new fitting procedure involving two quadrupole split absorptions (d_1 and d_{11}) was adopted to account for the Fe^{3+} ions in tetrahedral coordination, plus the quadrupole split absorption *a* characterizing the iron in octahedral coordination. The χ^2 values were lower (Table 2) and the area ratios of the absorption representing the *a* and *d* sites for the materials with $x = 0$ and 1 were closer to those expected ($I_{tetra}/I_{octa} = 0.33$ and 0.50, respectively). The area ratios of the absorption representing the *a* and *d* sites in the materials with $x = 2$ and 3 were different from the values expected if all the Ga^{3+} ions occupied the tetrahedral positions within the garnet framework (1 and 0, respectively). It is known (2) that the Sb^{5+} ions prefer octahedral sites and that Ga^{3+} ions prefer tetrahedral sites, although for high gallium concentrations the Ga^{3+} ions can also occupy the octahedral sites (2, 6–10). It follows from our data that in the materials with $x = 2$ and 3 some Ga^{3+} ions occupy the octahedral sites and, if it is assumed that equal recoil-free fractions pertain to both the octahedral and tetrahedral sites, the respective compounds adopt the formulation $\{YCa_2\}$

TABLE 1
^{57}Fe Mössbauer Parameters Obtained by Fitting the Spectra Recorded at 298 K from Compounds of Composition $YCa_2SbFe_{4-x}Ga_xO_{12}$ ($x = 0 - 3$) to One *d* and One *a* Doublet

	Site	δ (mms^{-1})	Δ (mms^{-1})	Γ (mms^{-1})	Area (%)	A_{oct}/A_{tet}	χ^2
$YCa_2SbFe_4O_{12}$	*d*	0.18(4)	1.24(2)	0.38(2)	79		
	a	0.38(4)	0.39(3)	0.30(4)	21		
						0.27	6
$YCa_2SbGaFe_3O_{12}$	*d*	0.18(4)	1.26(2)	0.38(2)	70		
	a	0.38(4)	0.38(3)	0.30(4)	30		
						0.43	4.7
$YCa_2SbGaFe_2O_{12}$	*d*	0.19(4)	1.28(2)	0.37(2)	59		
	a	0.38(4)	0.35(3)	0.32(4)	41		
						0.70	1.8
$YCa_2SbGa_3FeO_{12}$	*d*	0.20(4)	1.28(2)	0.39(2)	49		
	a	0.38(4)	0.32(3)	0.35(4)	51		
						1.02	1.3

$[Fe_{0.88}SbGa_{0.12}](Fe_{1.12}Ga_{1.88})O_{12}$ and $\{YCa_2\}[Fe_{0.52}SbGa_{0.48}](Fe_{0.48}Ga_{2.52})O_{12}$. However, this approximation must be treated with caution when considering data recorded at room temperature (11). In the latter material the fraction of Ga^{3+} ions in tetrahedral sites is ca. 0.8, which is larger than that found (2, 6) in the garnets of composition $Y_3Fe_{5-x}Ga_xO_{12}$. This difference may reflect the occupation by Sb^{5+} of octahedral sites which thereby decreases the probability of occupation of the octahedral sites by Ga^{3+} ions.

Although fairly good fits to the data were obtained by considering two doublets to account for the occupation of the tetrahedral *d* sites by the iron ions, the significant overlap between the different subspectra required that these parameters and peak area ratios be treated with caution. Thus a third fitting procedure, which involved the use of a distribution of quadrupole split absorptions to account for the *d* sites and a single doublet to account for the *a* sites, was adopted. This approach has been used (11) to fit the Mössbauer spectra of iron-titanium-containing

TABLE 2
^{57}Fe Mössbauer Parameters Obtained by Fitting the Spectra Recorded at 298 K from Compounds of Composition $YCa_2SbFe_{4-x}Ga_xO_{12}$ ($x = 0 - 3$) to Two *d* Doublets and One *a* Doublet

	Site	δ (mms^{-1})	Δ (mms^{-1})	Γ (mms^{-1})	Area (%)	A_{oct}/A_{tet}	χ^2
$YCa_2SbFe_4O_{12}$	d_1	0.17(3)	1.15(2)	0.32(3)	54		
	d_{11}	0.18(3)	1.46(2)	0.28(2)	22		
						0.32	4.5
	a	0.37(3)	0.38(3)	0.30(2)	24		
$YCa_2SbGaFe_3O_{12}$	d_1	0.18(3)	1.13(2)	0.29(3)	35		
	d_{11}	0.19	1.43(2)	0.30(2)	31		
						0.53	2.3
	a	0.37(3)	0.37(3)	0.32(2)	34		
$YCa_2SbGa_2Fe_2O_{12}$	d_1	0.19(3)	1.15(2)	0.30(2)	33		
	d_{11}	0.18(3)	1.45(2)	0.28(2)	23		
						0.79	1.3
	a	0.37(3)	0.35(3)	0.33(4)	44		
$YCa_2SbGa_3FeO_{12}$	d_1	0.18(3)	1.14(2)	0.37(2)	29		
	d_{11}	0.20(3)	1.42(2)	0.28(2)	19		
						1.08	1.1
	a	0.37(3)	0.31(3)	0.36(4)	52		

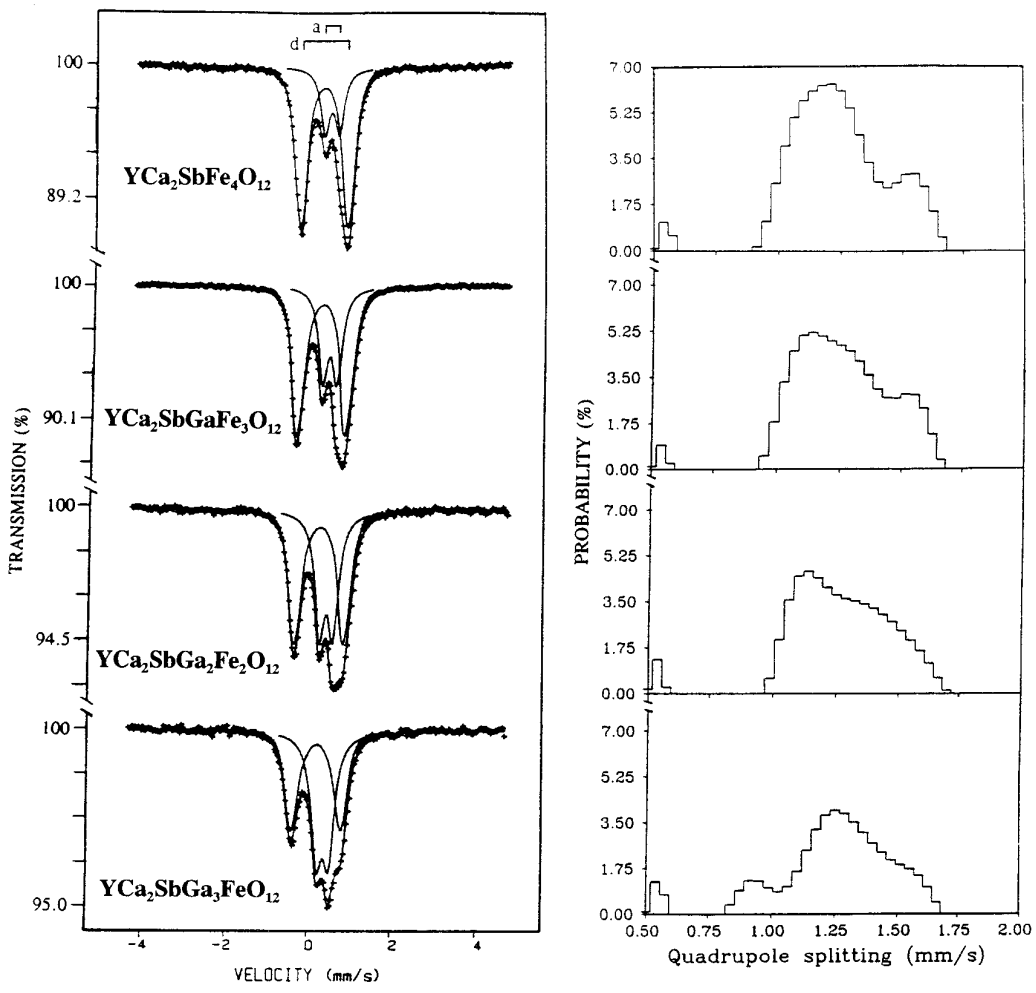

FIG. 2. Mössbauer spectra recorded at 298 K from $YCa_2SbFe_4O_{12}$, $YCa_2SbFe_3GaO_{12}$, $YCa_2SbFe_2Ga_2O_{12}$, and $YCa_2SbFeGa_3O_{12}$, when fitted to one doublet for the octahedral sites and a distribution of quadrupole splittings for the tetrahedral sites. The quadrupole splitting distribution is shown.

spinels. The χ^2 values were comparable, and in some cases remarkably lower, than in the previous fitting model. The results are shown in Fig. 2 and Table 3 and demonstrate that the isomer shifts of Fe^{3+} in both the *a* and *d* sites and the quadrupole splitting value of Fe^{3+} in the *a* sites are similar to those obtained from the fit using discrete lines. The quadrupole-splitting distributions for the *d*-sites obtained for the garnets $YCa_2SbFe_{4-x}Ga_xO_{12}$ ($x = 0 - 3$) (Fig. 2) are asymmetric, increasing rapidly from $\Delta = 0.80$ mms^{-1} to a broad maximum centered at 1.15–1.20 mms^{-1} and decreasing slowly as $\Delta = 1.70$ mms^{-1} is approached with a shoulder at $\Delta = 1.45$–1.50 mms^{-1}. The average values are consistent with those obtained from the three-doublet fit ($d_1 + d_{11} + a$). It can also be seen that as Ga^{3+} enters the garnet structure the probability of Δ_{max} decreases, i.e., the distributions become broader, which is also consistent with the trend observed in the relative areas of the *d* doublets obtained from the three-doublet fit (see Table 2).

b. $Y_{3-2x}Ca_{2x}Sb_xFe_{5-x}O_{12}$ ($x = 1.25, 1.5$). The ^{57}Fe Mössbauer spectra recorded at 298 K from the compounds of composition $Y_{3-2x}Ca_{2x}Sb_xFe_{5-x}O_{12}$ ($x = 1.25, 1.5$), in which the Fe^{3+} ions at the octahedral sites are replaced by Sb^{5+} ions (12), were fitted to the same models as were used to fit the spectra of the garnets of composition $YCa_2SbFe_{4-x}Ga_xO_{12}$ ($x = 0 - 3$). The fitting model involving a distribution of quadrupole split absorptions to account for the occupation of the *d* sites and a single doublet to account for the *a* sites was also found to be superior (Fig. 3). The quadrupole splitting distributions obtained for the compounds $Y_{3-2x}Ca_{2x}Sb_xFe_{5-x}O_{12}$ ($x = 1.25, 1.5$) (Fig. 3, Table 3) resemble those obtained from the garnet $YCa_2SbFe_4O_{12}$ except for the existence of another maximum at $\Delta \sim 0.75$–0.80 mms^{-1}. The quadrupole splitting contribution around this maximum is most distinctive in the case of the garnet in which $x = 1.5$. In this respect it is interesting to note that the three-doublet fit to the spectrum of this garnet gave a quadrupole splitting for one of the *d* doublets of

TABLE 3

^{57}Fe Mössbauer Parameters Obtained by Fitting the Data Recorded from Compounds of Composition $YCa_2SbFe_{4-x}Ga_xO_{12}$ ($x = 0 - 3$), $Y_{3-2x}Ca_{2x}Sb_xFe_{5-x}O_{12}$ ($x = 1.25, 1.5$), $Y_{3-x}Ca_xSn_xFe_{5-x}O_{12}$ ($x = 1.2$) and $NaCa_2Sb_2FeGa_2O_{12}$ to a Distribution of Quadrupole Split Absorptions for the Tetrahedral (d) Sites

Garnet	δ^a (mms^{-1})	Δ^a(mms^{-1})	Γ^a (mms^{-1})	Area^a (%)	δ^d (mms^{-1})	$\langle\Delta^d\rangle$ (mms^{-1})	Area^d (%)	χ^2
$YCa_2SbFe_4O_{12}$	0.37	0.38	0.29	24	0.18	1.24	76	3.2
$YCa_2SbFe_3GaO_{12}$	0.37	0.37	0.30	33	0.18	1.26	67	2.8
$YCa_2SbFe_2Ga_2O_{12}$	0.37	0.35	0.32	43	0.18	1.26	57	1.4
$YCa_2SbFeGa_3O_{12}$	0.37	0.31	0.35	52	0.18	1.25	48	0.9
$Y_{0.5}Ca_{2.5}Sb_{1.25}Fe_{3.75}O_{12}$	0.37	0.31	0.30	20	0.18	1.21	80	1.4
$Ca_3Sb_{1.5}Fe_{3.5}O_{12}$	0.38	0.24	0.29	16	0.19	1.16	84	2.7
$Y_2CaSnFe_4O_{12}$	0.38	0.43	0.24	19	0.17	1.09	81	2.5
$YCa_2Sn_2Fe_3O_{12}$	—	—	—	—	0.17	1.01	100	2.0
$NaCa_2Sb_2FeGa_2O_{12}$	—	—	—	—	0.18	0.84	100	0.8

Note. $\langle\Delta^d\rangle$, Average quadrupole splitting of the distribution.

0.77 mms^{-1}, which correlates well with the value of 0.76 mms^{-1} at which this maximum appears. The results also show that there is a significant contribution of values centered about 0.80 mms^{-1} in the distribution obtained for the garnet with $x = 1.25$, which was not observed when fitting three discrete doublets to this spectrum.

c. $Y_{3-x}Ca_xSn_xFe_{5-x}O_{12}$ ($x = 1, 2$). The Mössbauer spectra recorded at 298 K from the tin-containing garnets $Y_{3-x}Ca_xSn_xFe_{5-x}O_{12}$ ($x = 1, 2$) are presented in Fig. 4, and the results of the fitting involving a distribution of doublets for the d sites were found to be superior to other fits to the data. The quadrupole splitting data obtained from the tin-containing garnets showed different trends from those recorded from the compounds $YCa_2SbFe_{4-x}Ga_xO_{12}$ (Fig. 4, Table 3). The distribution corresponding to the garnet $Y_2CaSnFe_4O_{12}$ was also asymmetric but the shoulder appeared on the lower side of the Δ values (ca. 0.95–0.98 mms^{-1}) and the maximum appeared at 1.18 mms^{-1}. These values correlate quite well with those obtained from the fitting procedure using discrete doublets. The distribution for the garnet $YCa_2Sn_2Fe_3O_{12}$ showed two clearly distinguishable maxima, one appearing at $\Delta = 0.84$ mms^{-1} and

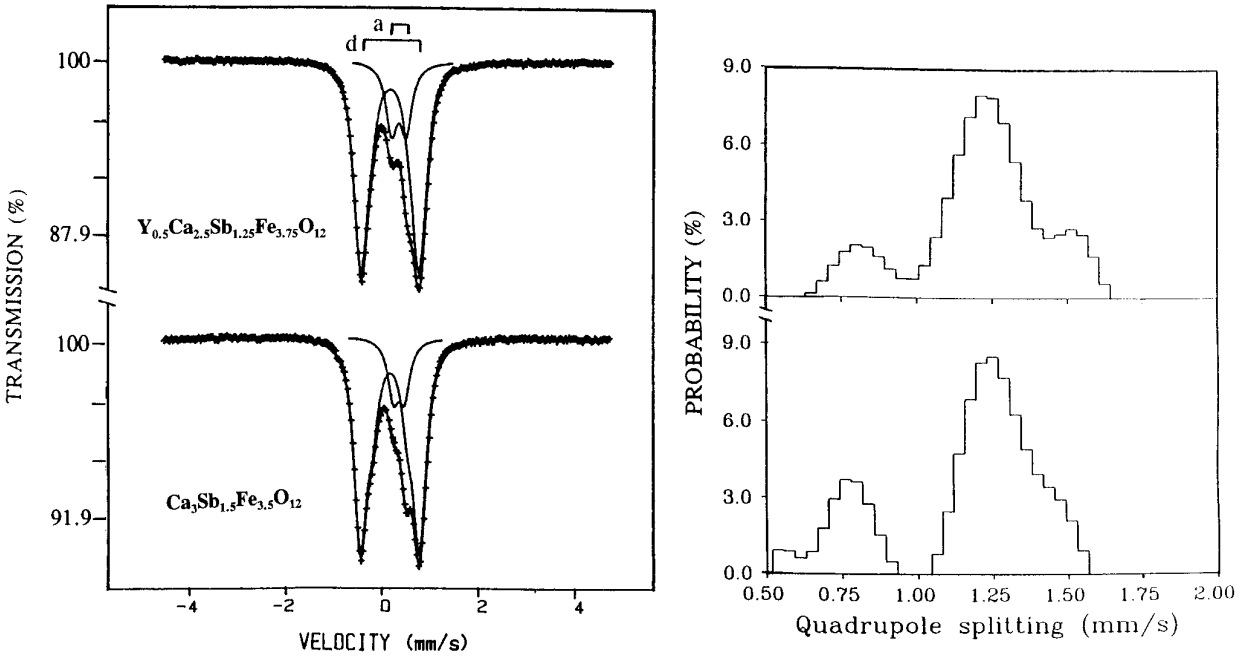

FIG. 3. Mössbauer spectra recorded at 298 K from $Y_{0.5}Ca_{2.5}Sb_{1.5}Fe_{3.75}O_{12}$ and $Ca_3Sb_{1.5}Fe_{3.5}O_{12}$, when fitted to one doublet for the octahedral sites and a distribution of quadrupole splittings for the tetrahedral sites. The quadrupole splitting distribution is shown.

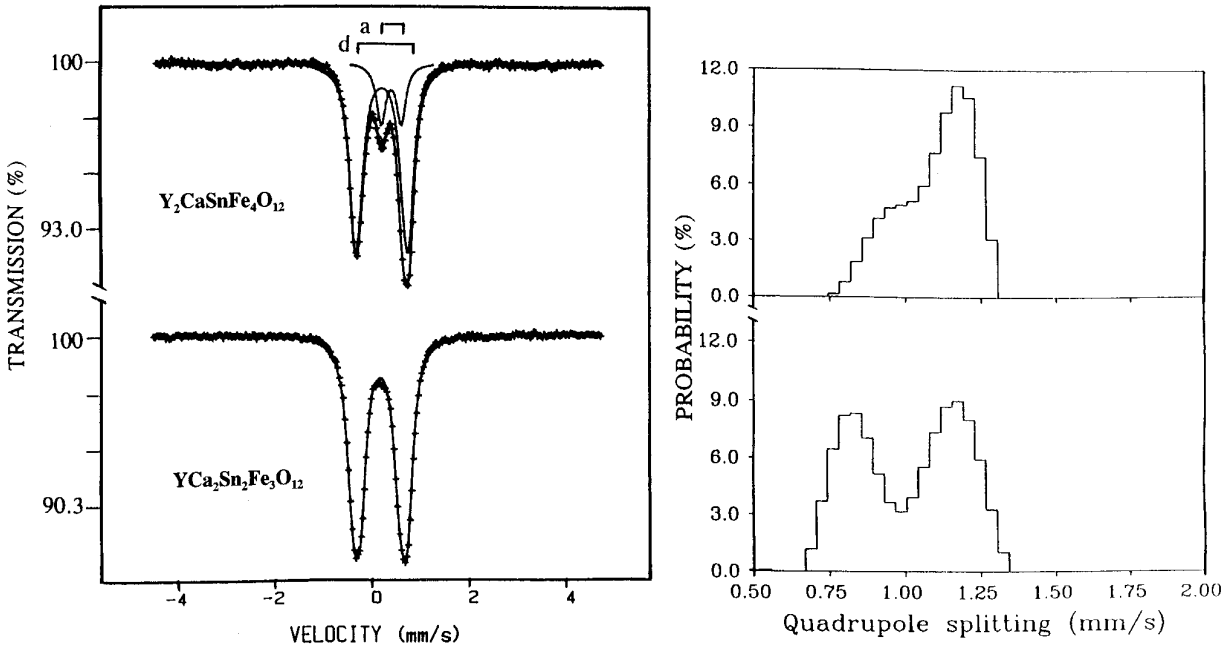

FIG. 4. Mössbauer spectra recorded at 298 K from $Y_2CaSnFe_4O_{12}$ and $YCa_2Sn_2Fe_3O_{12}$, when fitted to one doublet for the octahedral sites and a quadrupole splitting distribution for the tetrahedral sites.

another at $\Delta = 1.18$ mms^{-1} which is also in very good agreement with the discrete doublet fit.

d. $NaCa_2Sb_2FeGa_2O_{12}$. It is interesting to compare the preceeding results with those obtained from the garnet $NaCa_2Sb_2FeGa_2O_{12}$. The fitting of the spectrum recorded at 298 K from the compound $NaCa_2Sb_2FeGa_2O_{12}$ to a single *d* doublet, $\delta = 0.18$ mms^{-1}, $\Delta = 0.85$ mms^{-1}, gave an excellent χ^2 value of 1.1. The fitting of the data using a distribution of quadrupole splittings ($\chi^2 = 0.8$) gave a symmetrical distribution with an average value of $\Delta = 0.84$ mms^{-1} (Fig. 5). Hence, in this case the fit to a single doublet for the *d* sites appears to provide all relevant information.

From the results obtained here it can be concluded that, in the case of the garnets $YCa_2SbFe_{4-x}Ga_xO_{12}$ ($x = 0 - 3$), $Y_{3-2x}Ca_{2x}Sb_xFe_{5-x}O_{12}$ ($x = 1.25, 1.5$), and $Y_{3-x}Ca_xSn_xFe_{5-x}O_{12}$ ($x = 1, 2$), (i) the spectra recorded at 298 K are not suitably fitted by considering only one single doublet to account for the *d* sites, and (ii) although a fit considering two *d* doublets is more adequate, the use of a distribution of quadrupole splittings to account for the *d* sites provides a better description of the paramagnetic spectra and provides information which is difficult to extract when using fitting procedures involving discrete doublets. The existence of several contributions to the distribution of quadru-

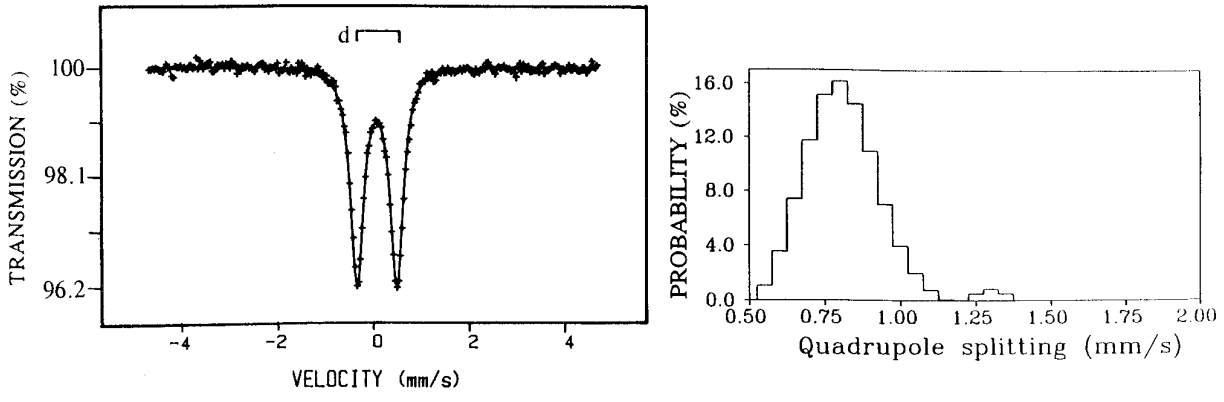

FIG. 5. Mössbauer spectrum recorded at 298 K from $NaCa_2Sb_2FeGa_2O_{12}$, when fitted to a quadrupole splitting distribution.

TABLE 4
Lattice and Mössbauer Parameters of Some Iron-Containing Garnets at Room Temperature

Garnet	a (Å)	δ^a (mms^{-1})	Δ^a (mms^{-1})	δ^d (mms^{-1})	Δ^d (mms^{-1})	Ref.
$Y_3Fe_5O_{12}$	12.386	0.38	0.47	0.16	0.97	[15]
$Sm_3Fe_5O_{12}$		0.41	0.34	0.16	0.83	[16]
$Gd_3Fe_5O_{12}$		0.42	0.38	0.16	0.89	[16]
$Dy_3Fe_5O_{12}$		0.38	0.49	0.16	0.90	[16]
$Yb_3Fe_5O_{12}$		0.40	0.50	0.15	0.99	[16]
$Lu_3Fe_5O_{12}$		0.39	0.57	0.20	0.95	[16]
$Tb_3Fe_5O_{12}$		0.36	0.37	0.15	0.87	[17]
$Y_3Fe_3Ga_2O_{12}$	12.347	0.37	0.37	0.15	0.87	[8]
$Y_3Fe_{2.2}Ga_{2.8}O_{12}$	12.327	0.39	0.39	0.12	0.93	[18]
$Y_3FeGa_4O_{12}$	12.308	0.37	0.32	0.15	1.01	[8]
$Y_3Fe_3Al_2O_{12}$	12.245	0.41	0.42	0.13	0.97	[7]
$Y_3Fe_2Al_3O_{12}$	12.176	0.41	0.38	0.12	0.99	[7]
$Y_3FeAl_4O_{12}$	12.091	0.42	0.33	0.09	0.97	[7]
$Y_3FeGaAl_3O_{12}$		0.39	0.38	0.10	0.95	[18]
$Ca_3Fe_2Ti_{1.42}Si_{1.58}O_{12}$		0.40	0.75	0.20	1.15	[19]
$Y_{2.5}Ca_{0.5}Sn_{0.5}Fe_{4.5}O_{12}$		0.42	0.48	0.14	0.99	[20]
$Y_2CaSnFe_4O_{12}$		0.42	0.52	0.14	1.06	[20]
$Y_{1.5}Ca_{0.5}Sn_{1.5}Fe_{3.5}O_{12}$		0.44	0.49	0.15	1.04	[20]
$YCa_2Sn_2Fe_3O_{12}$				0.16	1.02	[20]
$GdCa_2Sn_2Fe_3O_{12}$	12.666			0.17	0.97	[21]
$Ca_3Zr_2Fe_2SiO_{12}$	12.610			0.18	1.04	[15]
$YCa_2Zr_2Fe_2AlO_{12}$	12.618			0.17	1.09	[15, 18]
$Ca_3ZrSbFe_3O_{12}$	12.669			0.23	0.99	[3]
$Ca_3SnSbFe_3O_{12}$	12.634			0.22	0.96	[3]
$NaCa_2Sb_2Fe_3O_{12}$	12.600			0.22	0.51	[3]
$Na_3Te_2Fe_3O_{12}$	12.524			0.23	0.51	[15]
$Ca_3Fe_2Ge_3O_{12}$	12.320	0.39	0.35			[22]
$Ca_3FeAlGe_3O_{12}$	12.205		0.31			[22]
$Ca_3FeInGe_3O_{12}$	12.475		0.45			[22]
$CdFe_2Ge_3O_{12}$	12.263	0.38	0.26			[22]
$Ca_3Fe_2Si_3O_{12}$	12.070	0.41	0.59			[23]
$Mn_3Fe_2Si_3O_{12}$	11.821	0.39	0.34			[23]
$Cd_3Fe_2Si_3O_{12}$		0.38	0.57			[23]

Note. δ values are referred to metallic iron. Superscript a refers to octahedral sites. Superscript d refers to tetrahedral sites.

pole splitting can be understood by appreciating that the FeO_4 tetrahedra share corners with octahedra in which the cations can be Sb^{5+} or Fe^{3+} or Ga^{3+} or Sn^{4+}. In addition, two of the tetrahedral edges are shared (13) with dodecahedra in which the cations can be Y^{3+} or Ca^{2+}. The random distribution of these different cations, in different charge states, over the octahedral and dodecahedral sites of the garnet structure affects the electric field gradient at the tetrahedral sites and leads to different quadrupole splittings depending on the different neighboring configurations of the FeO_4 tetrahedra. The results demonstrate the sensitivity of the Mössbauer parameters to changes in the environment of iron when the immediate oxygen coordination remains unchanged. Such an effect was first observed in other minerals some time ago (14).

The magnitude of the Mössbauer parameters recorded from the compounds examined here may be best considered by comparison with data taken from the literature pertaining to Fe^{3+} in garnets, which are collected in Table 4. It is clear that the a sites are characterized by small values of Δ, indicative of regular octahedral coordination, while the d sites are characterized by low isomer shifts and large quadrupole splittings, indicating that the coordination of Fe^{3+} in the tetrahedral sites is more distorted than that of the Fe^{3+} ions in the octahedral sites (19). The low isomer shifts and large quadrupole splittings of the d sites have sometimes (16, 21, 24) been interpreted in terms of the covalency of the tetrahedral Fe^{3+}–oxygen bonds. The electron transfer from the oxygen p-orbitals into the tetrahedral Fe^{3+} $3d$- and $4s$- orbitals appears to be reflected in a decrease in δ due to increased s- electron density at the nucleus. The increase in Δ arises from the electron transfer to the $3d$ orbitals which deforms the symmetry of the $3d$ electron charge density and results in a significant eq_{val} contribution which adds to the dominant eq_{latt} contribution to the electric field gradient. This interpretation is supported (25) by polarized neutron diffraction studies of $Y_3Fe_5O_{12}$ which show a significant spin transfer between

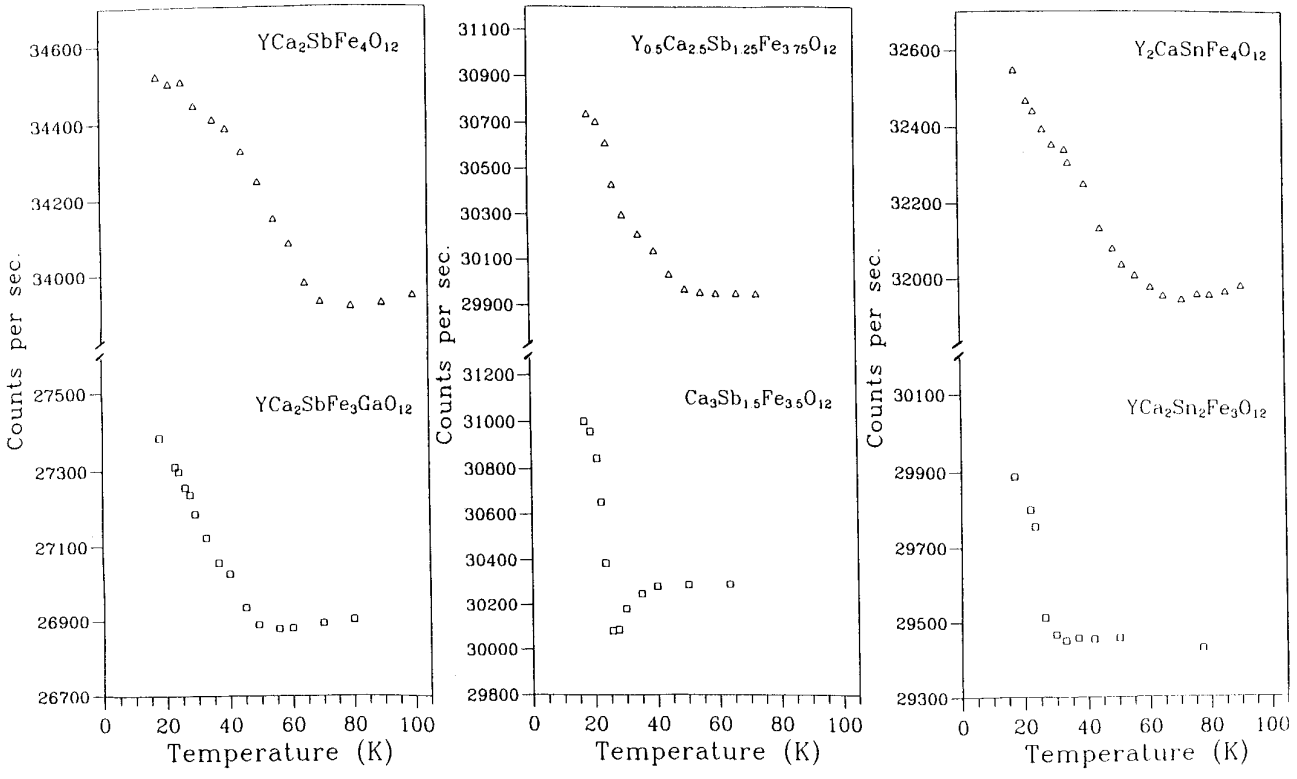

FIG. 6. Thermoscanning data from which the magnetic ordering temperatures of the garnets were determined.

oxygen and tetrahedral Fe^{3+}. Similar covalency effects have also been observed (25) in other rare earth iron garnets.

In the materials examined here the Mössbauer parameters of the Fe^{3+} ions located on the octahedral sites of the garnets $YCa_2SbFe_{4-x}Ga_xO_{12}$ ($x = 0 - 3$) and $Y_{3-2x}Ca_{2x}Sb_xFe_{5-x}O_{12}$ ($x = 1.25, 1.5$) are similar to those observed in the garnets $Y_3Fe_{3-x}Ga_{2+x}O_{12}$ (Table 4). However the δ values of the tetrahedral Fe^{3+} ions in the antimony-containing garnets, although low, are larger than those of tetrahedral Fe^{3+} in most of the garnets listed in Table 4 (see, for example, the δ values of the gallium-containing garnets $Y_{3-2x}Fe_{3-x}Ga_{2+x}O_{12}$), therefore suggesting that the covalency effects present in all these garnet systems are smaller in the compounds studied in this paper. In contrast, the Δ values of the compounds examined here are considerably larger: the existence of tetrahedral Fe^{3+} environments which give rise to quadrupole splitting distributions of ca. 1.45 mms^{-1} in iron-containing garnets is unprecedented (in Table 4, the largest Δ value, which corresponds to the titanium-andradite $Ca_3Fe_2Ti_{1.42}Si_{1.58}O_{12}$, is 1.15 mms^{-1}). Hence, in the antimony-containing garnets examined here although some contribution from eq_{val} to the quadrupole splitting due to covalency effects is reasonable, the eq_{latt} contribution must be much larger probably due to the existence of highly distorted FeO_4 tetrahedra.

It is interesting to note that the literature Mössbauer parameters of the tin-containing garnets $Y_{3-x}Ca_xSn_xFe_{5-x}O_{12}$ ($x = 1, 2$) (Table 4) correlate well with the average parameters obtained here from fitting our spectra to a distribution of quadrupole splittings (see Table 3). Although the literature does not consider (20) the possible existence of more than two tetrahedral sites in these compounds, the previous data were presented (20) without the fitted lines and without details of the fitting procedure or the goodness of the fits. It seems that more structural data are necessary to confirm the existence of the different tetrahedral sites.

Magnetic Interactions

Thermoscanning experiments showed the garnets $YCa_2SbFe_4O_{12}$ and $YCa_2SbFe_3GaO_{12}$ to magnetically order below 75 and 52 K, respectively (Fig. 6). The garnets $YCa_2SbFe_2Ga_2O_{12}$ and $YCa_2SbFeGa_3O_{12}$ remained paramagnetic at 18 K. The ^{57}Fe Mössbauer spectra recorded at 18 K from these compounds are shown in Fig. 7. The spectrum recorded from $YCa_2SbFe_4O_{12}$ showed a well-defined magnetic pattern and was fitted to one sextet (a) corresponding to Fe^{3+} in octahedral sites and five sextets ($d_1, \ldots, d_5$) corresponding to Fe^{3+} in tetrahedral sites. In this compound, all the tetrahedral sites are occupied by Fe^{3+} but half the octahedral sites are occupied by Fe^{3+} and half by Sb^{5+}. Each octahedral Fe^{3+} is linked through oxygen to six tetrahedrally coordinated Fe^{3+} such that all the octa-

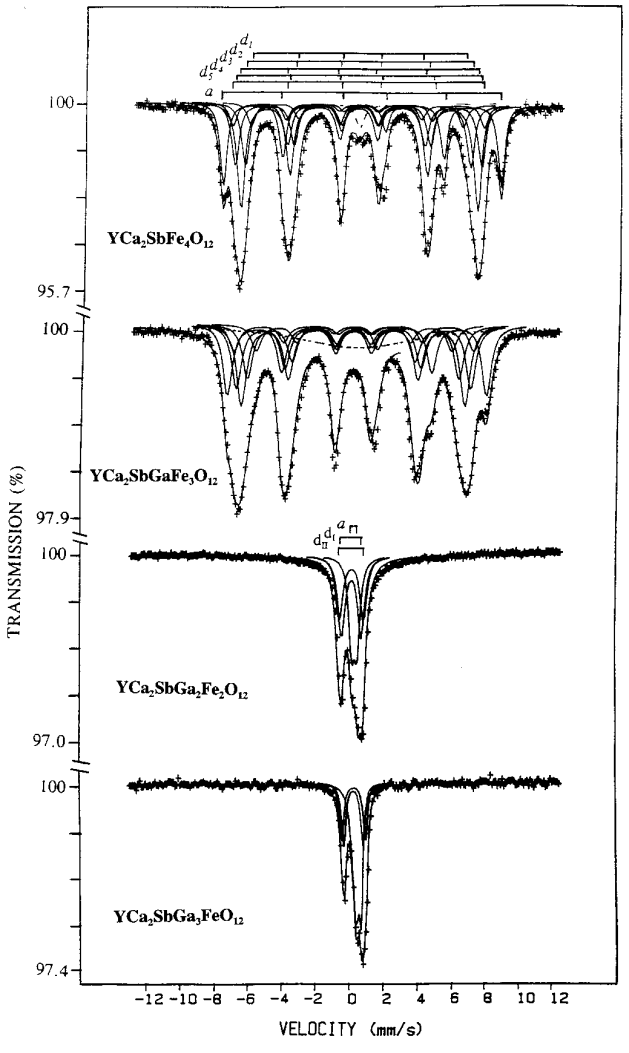

FIG. 7. Mössbauer spectra recorded at 18 K from $YCa_2SbFe_4O_{12}$, $YCa_2SbFe_3GaO_{12}$, $YCa_2SbFe_2Ga_2O_{12}$, and $YCa_2SbFeGa_3O_{12}$. The small absorption observed at $\delta \sim 0$ mms^{-1} in the top spectrum results from iron impurity in the aluminium foil which was used to sandwich the sample in the cryostat.

hedral sites have identical environments. However, the tetrahedrally coordinated Fe^{3+} ions are linked to four octahedral sites containing a statistical (binomial) distribution of Fe^{3+} and Sb^{5+} ions. In this way, five nonequivalent tetrahedral sites are expected, corresponding to the following configurations of neighboring octahedra:

$$4Fe^{3+};\quad 3Fe^{3+} + 1Sb^{5+};\quad 2Fe^{3+} + 2Sb^{5+};$$
$$1Fe^{3+} + 3Sb^{5+};\quad 4Sb^{5+}.$$

Hence the data were fitted to this model (26) and the results are shown in Table 5. The relative intensities calculated by assuming equal recoil-free fractions for all the different sites are in satisfactory agreement with those expected for a random distribution of Fe^{3+} and Sb^{5+} over the octahedral sites (4.5, 19, 28, 19, and 4.5% for the tetrahedral sites and 25% for the octahedral site). The average value of the tetrahedral field (435 kG) is comparable with the extrapolated field values at 0 K of the garnets $NaCa_2Sb_2Fe_3O_{12}$ and $Ca_3ZrSbFe_3O_{12}$ (447 and 450 kG, respectively), which also contain Sb^{5+} at the octahedral sites (3).

The magnetic contributions to the spectrum recorded from $YCa_2SbFe_3GaO_{12}$ at 18 K were less well resolved than those obtained from $YCa_2SbFe_4O_{12}$ (Fig. 7). Since the spectrum showed the occurrence of significant relaxation, it was fitted to one *a* sextet and five *d* sextets plus a broad band to account for the observed relaxation in the center of the spectrum. The values of the octahedral and average tetrahedral fields (487 and 415 kG, respectively) obtained from the fit are smaller than those observed in $YCa_2SbFe_4O_{12}$ (Table 5). The results are indicative of the frustration of magnetic order resulting from the partial substitution of tetrahedrally coordinated Fe^{3+} by diamagnetic Ga^{3+}.

The spectra recorded at 18 K from $YCa_2SbFe_2Ga_2O_{12}$ and $YCa_2SbFeGa_3O_{12}$ showed no evidence of magnetic order and were composed of paramagnetic doublets (Fig. 7, Table 5). The broader spectral lines of $YCa_2SbFe_2Ga_2O_{12}$, as compared with those of $YCa_2SbFeGa_3O_{12}$, are indicative of the compound being close to the onset of magnetic ordering. In these two compounds, the partial substitution of Fe^{3+} by diamagnetic Ga^{3+} at both the octahedral and tetrahedral sites results in a significant dilution of the magnetic moments in both sublattices and a weakening of the *a–d*, *d–d*, and *a–a* antiferromagnetic interactions. This is reflected in the considerable reduction of the mag-

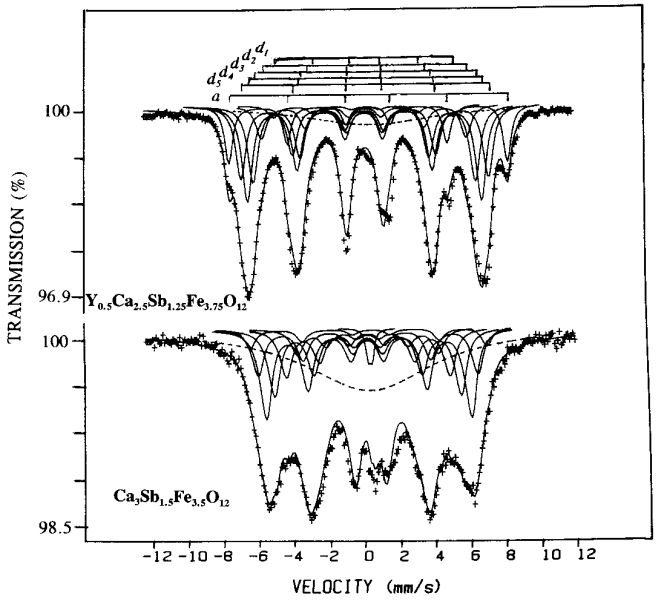

FIG. 8. Mössbauer spectra recorded at 18 K from $Y_{0.5}Ca_{2.5}Sb_{1.25}Fe_{3.75}O_{12}$ and $Ca_3Sb_{1.5}Fe_{3.5}O_{12}$.

TABLE 5
^{57}Fe Mössbauer Parameters Obtained from the Spectra Recorded at 18 K from Compounds of Composition $YCa_2SbFe_{4-x}Ga_xO_{12}$

	Site	δ (mms^{-1})	Δ (mms^{-1})	Γ (mms^{-1})	H (kG)	Area (%)
$YCa_2SbFe_4O_{12}$	d_1	0.31(2)	−0.17(1)	0.56(3)	392	6.5
	d_2	0.31(2)	−0.09(2)	0.56(3)	417	18
	d_3	0.31(2)	0.04(2)	0.56(3)	437	30
	d_4	0.31(2)	−0.03(2)	0.56(3)	456	18
	d_5	0.31(2)	−0.03(2)	0.56(3)	465	6.5
	a	0.31(3)	−0.05(1)	0.49(3)	514	21
$YCa_2SbGaFe_3O_{12}$	d_1	0.31(2)	0.04(1)	0.71(3)	365	8
	d_2	0.31(2)	−0.01(2)	0.71(3)	395	17
	d_3	0.31(2)	0.00(2)	0.71(3)	417	26
	d_4	0.31(2)	−0.04(2)	0.71(3)	438	20
	d_5	0.31(2)	−0.04(2)	0.71(3)	448	8
	a	0.53(3)	0.02(1)	0.68(3)	484	21
$YCa_2SbGa_2Fe_2O_{12}$	d_1	0.24(5)	1.15(3)	0.49(2)		38
	d_{11}	0.24(5)	1.41(3)	0.49(2)		30
	a	0.43(5)	0.32(3)	0.40(2)		32
$YCa_2SbGa_3FeO_{12}$	d_1	0.29(5)	1.11(3)	0.30(2)		25
	d_{11}	0.31(5)	1.39(3)	0.30(2)		22
	a	0.43(5)	0.32(3)	0.35(2)		53

Note. Δ is the quadrupole shift.

netic ordering temperatures as compared to that observed in $YCa_2SbFe_4O_{12}$.

Thermoscanning measurements (Fig. 6) showed the magnetic ordering temperatures of the compounds $Y_{0.5}Ca_{2.5}Sb_{1.25}Fe_{3.75}O_{12}$ and $Ca_3Sb_{1.5}Fe_{3.5}O_{12}$ to be 50 and 25 K, respectively. The Mössbauer spectra recorded from these compounds at 18 K are presented in Fig. 8. The spectrum recorded from the compound $Y_{0.5}Ca_{2.5}Sb_{1.25}Fe_{3.75}O_{12}$ was best fitted to one *a*- and five *d*-magnetic components with hyperfine magnetic fields of 518 (octahedral sites) and 426 kG (average tetrahedral sites), respectively (Table 6). The results show that the substitution of ca. 25% of the Fe^{3+} located in the octahedral sites by Sb^{5+} is accompanied by a decrease in the magnetic ordering temperature of ca. 25 K with respect to that of $YCa_2SbFe_4O_{12}$. The Mössbauer spectrum recorded at 18 K from the compound $Ca_3Sb_{1.5}Fe_{3.5}O_{12}$ showed (Fig. 8) the presence of significant relaxation, indicative of incomplete magnetic ordering. The average values for the hyperfine magnetic field at both the octahedral and tetrahedral sites at this temperature were estimated as ca. 439 and 353 kG, respectively. The substitution of 50% of the Fe^{3+} ions by Sb^{5+} in the octahedral sites is therefore reflected by a decrease in the magnetic ordering temperature of about 50 K as compared to that for $YCa_2SbFe_4O_{12}$.

The thermoscanning data recorded from the compound $Y_2CaSnFe_4O_{12}$ (Fig. 6), where 50% of the octahedral sites are occupied by Fe^{3+} and the other 50% by Sn^{4+} and all the tetrahedral sites are occupied by Fe^{3+}, showed the magnetic ordering temperature to be ca. 70 K. This value is very similar to that obtained for the compound $YCa_2SbFe_4O_{12}$. The Mössbauer spectrum recorded at 18 K (Fig. 9) was very similar to that recorded from $YCa_2SbFe_4O_{12}$ and was fitted to a similar model (*vide supra* and Table 7). The magnetic ordering temperature of 70 K for the garnet $Y_2CaSnFe_4O_{12}$ is much smaller than that found (27) by susceptibility measurements for other tin-substituted rare earth iron garnets such as $Dy_2CaSnFe_4O_{12}$ (280 K), $Er_2CaSnFe_4O_{12}$ (275 K), or $Yb_2CaSnFe_4O_{12}$ (270 K). However, the Mössbauer spectra recorded at 80 K from these garnets (27) did not show well-resolved magnetic patterns and were interpreted in terms of the presence of short-range magnetically ordered clusters. This interpretation has also been used to explain the observation that a doublet and a magnetic sextet coexist over a large range of temperatures in the Mössbauer spectra recorded below the magnetic ordering temperature of some diamagnetically substituted iron-containing garnets (25), as well as some magnetically dilute spinels (11). It has been suggested (28–30) that in the temperature range where the doublet and the magnetically-split spectral components coexist the crystal is composed of magnetically independent regions (superparamagnetic clusters) and that the larger regions are stable and responsible for the magnetically-split spectral component. The smaller regions are considered to contain iron in clusters of short-range order and to give rise to the central doublet in the Mössbauer spectrum. We sug-

TABLE 6
^{57}Fe Mössbauer Parameters Obtained from the Spectra Recorded at 18 K from Compounds of Composition $Y_{3-2x}Ca_{2x}Sb_xFe_{5-x}O_{12}$ (x = 1.25, 1.5)

	Site	δ (mms^{-1})	Δ (mms^{-1})	Γ (mms^{-1})	H (kG)	Area (%)
$Y_{0.5}Ca_{2.5}Sb_{1.25}Fe_{3.75}O_{12}$	d_1	0.29(2)	−0.10(1)	0.73(3)	334	4
	d_2	0.29(2)	−0.04(2)	0.73(3)	381	10
	d_3	0.29(2)	−0.03(2)	0.73(3)	413	23
	d_4	0.29(2)	0.07(2)	0.73(3)	438	28
	d_5	0.29(2)	−0.02(2)	0.73(3)	460	22
	a	0.51(3)	−0.01(1)	0.57(3)	518	13
$Ca_3Sb_{1.5}Fe_{3.5}O_{12}$	d_1	0.28(2)	0.06(1)	0.85(3)	261	8
	d_2	0.28(2)	0.06(2)	0.85(3)	304	16
	d_3	0.28(2)	−0.03(2)	0.85(3)	346	22
	d_4	0.28(2)	0.06(2)	0.85(3)	380	30
	d_5	0.28(2)	0.06(2)	0.85(3)	408	16
	a	0.44(3)	−0.12(1)	0.75(3)	439	6
	a	0.44(2)	0.24(2)	0.32(3)		2

Note. δ means average hyperfine parameters of the d sites. Δ is the quadrupole shift.

gest that a similar interpretation can be used to explain the coexistence of the doublet and sextet patterns observed in the spectra recorded from some of the garnets examined here.

The thermoscanning experiments (Fig. 6) showed the magnetic ordering temperature of the compound $YCa_2Sn_2Fe_3O_{12}$ to be ca. 28 K. Hence the substitution of all the Fe^{3+} ions in the octahedral sites by Sn^{4+} decreases by 42 K the magnetic ordering temperature observed in $Y_2CaSnFe_4O_{12}$. The Mössbauer spectrum recorded at 18 K (Fig. 9) showed the presence of a magnetically split component and a quadrupole split absorption. The shape of the magnetic component clearly indicates the presence of several magnetic fields and the spectrum was tentatively fitted to three sextets plus a doublet. A broad band was also included to account for the significant relaxation observed at the centre of the spectrum. The parameters obtained from this fit (Table 7) indicated the hyperfine magnetic field at the tetrahedral sites to be significantly smaller than that in the compound $Y_2CaSnFe_4O_{12}$.

Finally we would comment that the compound $NaCa_2Sb_2FeGa_2O_{12}$ did not show evidence of magnetic ordering at 18 K. It is known (3) that the magnetic ordering temperature of the garnet $NaCa_2Sb_2Fe_3O_{12}$ is 47 K, hence the results show that the substitution of $\frac{2}{3}$ of the Fe^{3+} ions located in the tetrahedral sites by diamagnetic Ga^{3+} results in a noticeable weakening of the d–d antiferromagnetic interaction.

We conclude therefore that the results here on diamagnetic substitution and magnetic ordering in some iron-containing garnets can be summarized as follows:

(i) The compounds $YCa_2SbFe_4O_{12}$ and $Y_2CaSnFe_4O_{12}$,

TABLE 7
^{57}Fe Mössbauer Parameters Obtained from the Spectra Recorded at 18 K from Compounds of Composition $Y_{3-x}Ca_xSn_xFe_{5-x}O_{12}$ (x = 1, 2)

	Site	δ (mms^{-1})	Δ (mms^{-1})	Γ (mms^{-1})	H (kG)	Area (%)
$Y_2CaSnFe_4O_{12}$	d_1	0.27(2)	0.03(1)	0.56(3)	408	6
	d_2	0.27(2)	−0.06(1)	0.56(3)	427	20
	d_3	0.27(2)	0.08(2)	0.56(3)	446	28
	d_4	0.27(2)	−0.03(2)	0.56(3)	465	20
	d_5	0.27(2)	−0.03(2)	0.56(3)	485	6
	a	0.52(3)	−0.02(1)	0.57(3)	522	20
$YCa_2Sn_2Fe_3O_{12}$	d_1	0.27(3)	−0.40(2)	0.49(3)	364	13
	d_2	0.27(3)	−0.44(5)	0.34(3)	392	31
	d_3	0.27(3)	−0.40(2)	0.45(3)	411	45
	d_4	0.25(3)	1.06(2)	0.46(3)		11

Note. Δ is the quadrupole shift.

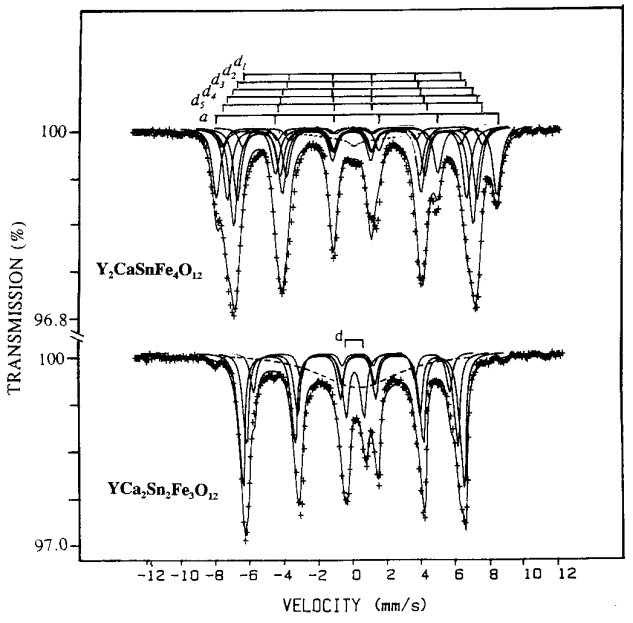

FIG. 9. Mössbauer spectra recorded at 18 K from $Y_2CaSnFe_4O_{12}$ and $YCa_2Sn_2Fe_3O_{12}$. The small amount of absorption observed at ~0 mms^{-1} in the top spectrum results from iron impurity in the aluminium foil which was used to sandwich the sample in the cryostat.

which have 50% of their octahedral sites and 100% of their tetrahedral sites occupied by Fe^{3+} ions, magnetically order at similarly high temperatures and show comparable octahedral and tetrahedral hyperfine magnetic fields at 18 K.

(ii) The substitution of Fe^{3+} ions by diamagnetic Sb^{5+} ions on the octahedral sites results in a considerable lowering of the magnetic ordering temperature. The compounds $Y_{0.5}Ca_{2.5}Sb_{1.25}Fe_{3.75}O_{12}$ and $Ca_3Sb_{1.5}Fe_{3.5}O_{12}$ show magnetic ordering on both the octahedral and tetrahedral sublattices at 18 K. A similar effect was observed in the compound $YCa_2SbFe_3GaO_{12}$ where 33% of the Fe^{3+} ions located at the tetrahedral sites are substituted by diamagnetic Ga^{3+} ions.

(iii) In the compounds $YCa_2SbFe_2Ga_2O_{12}$ and $YCa_2SbFeGa_3O_{12}$ the Ga^{3+} ions substitute the Fe^{3+} ions at both the octahedral and tetrahedral sites. The number of Fe^{3+} ions at the octahedral sites is comparable to that in the compounds of composition $Y_{0.5}Ca_{2.5}Sb_{1.25}Fe_{3.75}O_{12}$ and $Ca_3Sb_{1.5}Fe_{3.5}O_{12}$, but the number of Fe^{3+} ions at the tetrahedral sites is much lower resulting in the garnets being paramagnetic at 18 K. This result shows the importance of the *a–d* antiferromagnetic superexchange interaction. It seems that the dilution of the magnetic ions at the tetrahedral sites results in the frustration of magnetic ordering, not only in the *d* sublattice, but also in the *a* sublattice.

(iv) The compound $YCa_2Sn_2Fe_3O_{12}$, which does not contain Fe^{3+} ions in the octahedral sites, shows magnetic ordering below 42 K, indicating magnetic ordering on the *d* sublattice even in the absence of magnetic ions on the *a* sublattice. This implies that the *d–d* antiferromagnetic superexchange interaction is also important. The results recorded from the garnet $NaCa_2Sb_2FeGa_2O_{12}$ which does not contain Fe^{3+} ions at the octahedral sites and has $\frac{2}{3}$ of the tetrahedral sites occupied by Ga^{3+} ions shows that significant substitution of Fe^{3+} ions at the tetrahedral site induces frustration of the magnetic order.

ACKNOWLEDGMENTS

We thank the Commission of the European Communities for the award of a Fellowship (M.V.). We also thank The British Council and Ministerio de Education y Ciencia for an Acciones Integradas Award.

REFERENCES

1. A. F. Wells, "Structural Inorganic Chemistry," Fifth ed., p. 605. Clarendon, Oxford, 1984.
2. S. Geller, *Z. Kristall.* **125,** 47 (1967).
3. A. P. Dodokin, I. S. Lyubutin, B. V. Mill, and V. P. Peshkov, *Sov. Phys. JETP* **36,** 526 (1973).
4. I. S. Lyubutin, *in* "Proceedings, Conference on the Applications of the Mössbauer Effect, Tihany, 1969" (I. Dézsi, Ed.), p. 467. Akadémiai Kiadó, Budapest, 1971.
5. R. S. Preston, S. S. Hanna, and J. Herbele, *Phys. Rev.* **128,** 2207 (1962).
6. E. R. Czerlinsky, *Phys. Stat. Sol.* **34,** 483 (1969).
7. E. R. Czerlinsky and R. A. MacMillan, *Phys. Stat. Sol.* **41,** 333 (1970).
8. G. Amthauer, V. Günzler, S. S. Hafner, and D. Reinen, *Z. Kristall.* **161,** 167 (1982).
9. I. Nowik and S. Ofer, *Phys. Rev.* **153,** 409 (1967).
10. P. Röschmann, *J. Phys. Chem. Solids* **41,** 569 (1980).
11. R. E. Vandenberghe and E. de Grave, *in* "Mössbauer Spectroscopy Applied to Inorganic Chemistry," (G. J. Long and F. Grandjean, Eds.), Vol. 3, Chap. 3. Plenum, New York, 1989.
12. S. Geller, H. J. Williams, G. P. Espinosa, and R. C. Sherwood, *J. Applied Phys.* **33,** 542 (1964).
13. G. A. Novak and G. V. Gibbs, *Am. Mineral.* **56,** 791 (1971).
14. G. M. Bancroft, R. G. Burns, and A. G. Maddock, *Geochim. Cosmochim. Acta* **31,** 2219 (1967).
15. J. Sawicki and S. S. Hafner, *Phys. Lett.* **68A,** 80 (1978).
16. W. J. Nicholson and G. Burns, *Phys. Rev.* **133,** A1568 (1964).
17. G. N. Belozerskii, Y. P. Khimich, and V. N. Gitsovich, *Phys. Stat. Sol.* **79,** K125 (1977).
18. P. Köhler and G. Amthauer, *J. Solid State Chem.* **28,** 329 (1979).
19. G. Amthauer, H. Annersten, and S. S. Hafner, *Z. Kristall.* **143,** 14 (1976).
20. I. S. Lyubutin, E. F. Makarov, and V. A. Povitskii, *Sov. Phys. JETP* **26,** 44 (1967).
21. I. S. Lyubutin and A. P. Dodokin, *Sov. Phys. Cristall.* **15,** 936 (1971).
22. I. S. Lyubutin, L. M. Belyaev, R. Grzhikova, and I. Lipka, *Sov. Phys. Cristall.* **17,** 116 (1972).
23. H. Nishizawa, M. Shimada, K. Matsuoka, and M. Koizumi, *Bull. Chem. Soc. Japan* **50,** 3186 (1977).
24. R. M. Housley and R. W. Grant, *Phys. Rev. Lett.* **29,** 203 (1972).
25. M. Bonnet, A. Delapalme, H. Fuess, and P. Becker, *J. Phys. Chem. Solids* **40,** 863 (1979).
26. V. A. Bokov, S. I. Jushchuk, and G. V. Popov, *Solid State Commun.* **7,** 373 (1969).
27. M. Vaidya and P. H. Umadikar, *J. Phys. Chem. Solids* **52,** 827 (1991).
28. J. M. D. Coey, *Phys. Rev. B* **6,** 3240 (1972).
29. J. Piekosczewski and J. Suwalski, *in* "Proceedings, Conference on the Applications of the Mössbauer Effect, Tihany, 1969" (I. Dézsi, Ed.) p. 499. Akadémiai Kiadó, Budapest, 1971.
30. Y. Ishikawa, *J. Appl. Phys.* **35,** 1054 (1964).